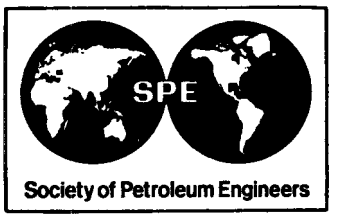

SPE 25257

Cleaning Up Spilled Gasoline With Steam: Compositional Simulations

A.E. Adenekan, Exxon Production Research Co., and T.W. Patzek,* U. of California

*SPE Member

This paper was prepared for presentation at the 12th SPE Symposium on Reservoir Simulation held in New Orleans, LA, U.S.A., February 28–March 3, 1993.

Abstract

A finite-difference compositional simulator has been developed and tested at U.C. Berkeley to model the flow of mixtures of Nonaqueous Phase Liquids (NAPLs) through the air zone and into aquifers. The simulator has been successfully used to history-match a steam injection pilot at a 'Clean Site' near the Lawrence Livermore National Laboratory in California -- a test site for the Gasoline Spill Area (GSA) cleanup pilot plannned for early '93. Because of its multicomponent capabilities, the simulator has been used to calculate (a) production rates of individual gasoline components in the GSA to size treatment facilities, (b) areal and vertical distribution of gasoline after the first cycle of steam injection, and (c) steam injection rate that limits growth of the steam zone beyond the cleanup area. It has been shown that gasoline present in the permeable sands and gravel layers can be successfully recovered by injecting steam into these layers in a 7-spot pattern. For the conditions assumed in the model, it will take less than 16 days to recover nearly all of the gasoline in the sands and gravel layers. By that time, the maximum aqueous concentrations of all hydrocarbon components in these layers will have dropped to less than 0.01 mg/l. The results show that vaporization, followed by bulk movement of the vapor to the production well is the dominant recovery mechanism. In terms of time required for cleanup, model results are most sensitive to permeability of the medium. Other parameters, such as the relative permeabilities and the number of components, also affect the outcome, but to a lesser extent.

Introduction

A compositional simulator M^2NOTS (*Multicomponent Non-isothermal Organics Transport Simulator)* has been developed [3,4] at U.C. Berkeley to model the flow of mixtures of Nonaqueous Phase Liquids (NAPLs) through the vadose zone and into aquifers. The NAPLs can have arbitrary densities, boiling temperatures, and viscosities. The M^2NOTS simulator is a major extension of an existing two-phase (water & gas), two-component (H_2O & air), and nonisothermal simulator TOUGH2, developed at the Lawrence Berkeley Laboratory [1,2] for geothermal applications. The M^2NOTS integrated finite-difference model is (a) three-dimensional; (b) fully implicit; (c) three-phase (aqueous, gaseous, and NAPL); (d) non-isothermal if needed; and (e) multicomponent (water, air, and any number of hydrocarbon components). The compositional and multiphase part of M^2NOTS has the following features: (a) each component of every phase in a grid block may partition into every other phase; (b) each phase in a grid block may appear or disappear; (c) the appearance or disappearance of a phase is established by a multicomponent, isothermal flash calculation performed at each iteration; and (d) the relative permeabilities are calculated from generalized power law equations for two-phase flow and the Stone II model for three-phase flow. The M^2NOTS well model can handle multiple fluid or heat injection wells on pressure or rate constraints, and fluid producers with variable pump levels and on deliverability or pump pressure constraints.

In the last twenty years, sophisticated thermal and compositional simulators have been developed to model oil reservoirs and it appears that these codes may also be used to study NAPL contamination problems. However, usually this is not the case because oil and NAPL transport and recovery are dominated by different mechanisms. For example, reservoir engineers are generally not interested in the relatively insignificant quantity of oil dissolved in the water phase; neither is diffusion considered important. On the other hand, dissolution and transport of organic compounds in the water phase, and diffusion of organic vapors in the gas phase may be quite important in NAPL contamination studies. Because oil reservoirs are generally deep and confined, oil industry simulators usually assume no-flux boundaries for a modeled domain. In subsurface contamination problems, we are generally dealing with shallow systems, and are usually interested in evaluating the exchange of contaminants between the subsurface and the atmosphere. Yet another example of how the differences in emphasis enter into code formulation is the treatment of appearance and disappearance of phases. Most oil reservoir codes assume that the oil phase cannot completely disappear from a grid block. This is justifiable because most crude oils contain heavy, nonvolatile components. In contrast, the goal of many remediation efforts is to completely remove a NAPL. Therefore, codes used to study transport of NAPLs need to be more flexible in dealing with the appearance and disappearance of phases. For example, the M^2NOTS model has a sophisticated algorithm for choosing the optimal sets of unknowns for all seven possible phase combinations (water, NAPL, Gas, Water + NAPL, Water + Gas, Gas + NAPL, Water + NAPL + Gas) and no component is required to have a 'master' phase to calculate its partitioning.

Initially, we validated [3,5] the M^2NOTS simulator with a laboratory, one-dimensional, two-component (benzene-toluene), water and steamflood data set [6]. We also used M^2NOTS to history-match a shallow steam injection pilot at a 'Clean Site' near the Lawrence Livermore National Laboratory [3,7] -- a test for the Gasoline Spill Area (GSA) cleanup project [7] to be started in early '93. Apart from the GSA, the Clean Site is perhaps the most extensively imaged and described subsurface volume in the world and, therefore, matching its response was a crucial test of the simulator. In the Clean Site simulation study, we have achieved good agreement with the field data, and matched (a) the injection and production rates, (b) the temperature histories at two monitoring wells, and (c) the steam breakthrough time at the production well.

Because the M^2NOTS simulator is compositional, we have used it to evaluate how effectively can we remove gasoline spilled at the GSA site by injecting steam. In particular, we have calculated (a) production rates of individual gasoline components to design treatment facilities), (b) areal and vertical distribution of gasoline after the first cycle of steam injection, and (c) steam injection rate that limits growth of the steam zone beyond the cleanup area.

Simulations of Gasoline Spill Area

Soil and groundwater contamination at the Lawrence Livermore National Laboratory Gasoline Spill Area (GSA) resulted from leaking underground storage tanks. The size of spill is not known and estimates range from 10,000 to over 100,000 gallons. It is known, however, that the gasoline was released from 1952 to 1979 and the leaking tanks were removed in 1980. Extensive field studies have been performed at this site over the last five years [8,9] to evaluate the extent of the contamination, and obtain an understanding of the hydrogeology of the site.

The GSA area is underlain by an unconsolidated, heterogeneous deposit of interbedded gravels, sands, silts and clays, as well as mixtures containing varying proportions of these soil types. Average static groundwater level at the site is about 30 meters below the ground surface. Below a depth of 40 meters, there is a continuous, low permeability silts and clays layer that is at least 9 meters thick in most places. Chemical analyses of soil and groundwater samples show that this layer is not contaminated and, therefore, we have limited our simulations to the soils above it. The bottom silts and clays unit is overlain by a uniformly thick (about 3 meters) layer of sands and gravels, designated as the Lower Aquifer. The Lower Aquifer in turn is overlain by another fairly continuous layer of silts and clays that is 3 to 5 meters thick at most locations. This unit is referred to as the Aquitard. Another sands and gravels unit, called the Upper Aquifer, extends above the Aquitard and is about 7.5 meters thick in the central section of the site. The location of the water table at the GSA is such that the lower 2 meters the Upper Aquifer is saturated. Overlying the Upper Aquifer is an 18-meter layer of silts and clays containing scattered zones of sandy and gravelly materials.

Non-aqueous phase gasoline is present both above and below the water table at the GSA. A 7.5-meter rise in the regional water table that occurred after the spill has

caused some gasoline to be trapped below the current water table. Data shows that most of the gasoline trapped below the water table is at the interface between the Lower Aquifer and the Aquitard. Contours of benzene concentrations in soil samples taken from the Lower Aquifer [13] are shown in Fig. 1. A significant portion of the gasoline trapped in the unsaturated zone has been removed by vacuum extraction operations that have been carried out in the last few years. In addition, biodegradation seems to be significant in the unsaturated zone with low residual gasoline saturation [7]. However, neither vacuum extraction nor biodegradation has significantly changed the conditions immediately above and below the water table. Thus, it has been decided [7] that steam injection coupled with vacuum extraction and electrical resistance heating will be used to recover the residual gasoline near and below the water table. Electrical heating will be used to heat up the Aquitard which, because of its low permeability, is not expected to be percolated by steam. Current plans call for six injection wells around the periphery of the spill and one production well in the center of the spill (Figs. 1 and 2). Steam will be injected into the Upper and Lower Aquifers while the Aquitard is electrically heated.

Figs. 3 and 4 show the vertical and plan view of the finite-difference mesh chosen for this study. We have idealized the proposed arrangement of injectors and producer as a seven-spot pattern and assumed that flow and transport within the pattern possess symmetry. Therefore, simulation of only one-twelfth of the pattern is required. The model consists of four horizontal layers: the Upper Aquifer, the Aquitard, and two layers that represent the Lower Aquifer. The Lower Aquifer has been divided into two layers to account for the difference in current gasoline saturations. The model layer representing the high gasoline saturation zone of the Lower Aquifer is 0.6 meter thick. The entire model consists of 506 grid blocks. The thick silts and clays layer above the Upper Aquifer and the one below the Lower Aquifer are the over- and underburden in the model. This is supported by results of the Clean Site simulations that showed minimal percolation of steam into the low permeability units that were included in that model [3,7].

Table 1 lists the soil properties in the Base Run. The permeability is based on the results of several pumping tests that have been performed at the site and ranked [13] as poor, fair, good, or excellent. Only the top two categories were used in obtaining the current estimates of permeability, but the results were scattered nevertheless. The more reliable ones yielded permeabilities between 0.5 and 40 darcies for the sands and gravels, with more than half of the data points falling between 1 and 7 darcies. Hence the value of 5 darcies was used in the Base Run. The silts and clays were assigned permeability of 10 millidarcy. The vertical to horizontal permeability ratio was set to one-tenth.

Field-measured relationships were not available for relative permeability and capillary pressure functions. Therefore, the Stone II model was used to calculate the three-phase relative permeabilities, while the gas-NAPL and NAPL-water capillary pressures were calculated from the modified van Genuchten's functions [10]. The parameters appearing in these functions have been assigned values based on literature data published for similar soil types.

The initial composition of the NAPL used in the model is based on the results of a laboratory analysis of a sample of the gasoline found at the site [13]. Because this analysis does not provide sufficient breakdown of the gasoline into its constituents (percentage concentrations are given for groups of compounds such as paraffins), it was necessary to use additional literature data on the composition of regular gasolines [11,12]. Because the computer CPU and storage requirements limit the number of components that can be included in a simulation model, three pseudocomponents were chosen to represent the spilled gasoline, benzene, p-xylene, and n-decane. The mixture consisted of 2.2 mole % of benzene, 74.1% of p-xylene, and 23.7% of n-decane. Despite its low mole fraction, benzene was included as a separate component because of its high solubility in water relative to other gasoline components and its importance as an environmental contaminant; p-xylene represented the C_7 - C_9 hydrocarbons, while n-decane the C_{10} - C_{12} hydrocarbons. In choosing pseudo components to represent the gasoline, other factors that might affect its transport were also taken into consideration [3]. Among these were the boiling point distribution curve, aqueous solubility, and viscosity.

Initial condition for the steam injection simulations was that of gravity-capillary equilibrium. The initial NAPL distribution (Fig. 5) reflected roughly the data from chemical analyses of soil and groundwater samples [13]. The total amount of NAPL initially in-place within the element of symmetry was 3,500 gallons (42,000 gallons within the entire 7-Spot pattern). As indicated earlier, no-flow conditions were imposed at the upper and lower boundaries, although heat losses to

the confining layers were allowed. Ambient temperature and equilibrium hydrostatic pressure were specified at the outer vertical boundary of the model.

Steam was injected into both the Upper and Lower Aquifer. The constant injection pressure was specified as 3.5×10^5 Pa and the quality of the injected steam was 90%. The production well was open to all layers and it produced on deliverability against a bottomhole pressure of 0.6×10^5 Pa, i.e., a pump vacuum of about 0.4 atmospheres. Each steam injection simulation was allowed to proceed until some time after steam breakthrough at the producer.

Results of the Base Run

Figs. 6-8 show the simulated recovery rates of benzene, p-xylene, and n-decane in the gas phase, the aqueous phase, and as part of a separate hydrocarbon (NAPL) phase. Recovery rates of all hydrocarbon components in both the gas and NAPL phase show two distinct peaks. Recovery rates of benzene and p-xylene in the water phase also show peaks, but they are less pronounced. These peak rates coincide with steam breakthrough at the producer in model layers that contained some NAPL initially. The first peak corresponds to steam breakthrough in the Upper Aquifer while the second one to breakthrough in the Lower Aquifer. Steam breakthrough at the producer occurs earlier in the Upper Aquifer than in the Lower Aquifer for two reasons: (i) steam is injected into the Upper Aquifer at a higher rate because the formation fluid pressure is lower than in the Lower Aquifer where the additional hydrostatic head adds to the pressure; and (ii) initially, the Upper Aquifer is only partially saturated with water and gas mobility is higher. Steam breakthrough occurs in the Upper Aquifer after about 7 days of steam injection while it takes about 12 days for breakthrough to occur in the Lower Aquifer.

The rate of recovery of each component as part of a hydrocarbon liquid phase is significant only for a short time interval immediately preceding steam breakthrough. Although the initial NAPL saturation is below residual everywhere, evaporation of hydrocarbon components into the steam zone and their condensation just ahead of the steam condensation front cause the local NAPL saturation to rise above residual and the NAPL be mobile. The locally higher NAPL saturation ahead of the steam condensation front is referred to as a NAPL bank. Another important feature of the results shown here is the overlap between the time interval during which there is significant recovery in the NAPL phase and the time interval of significant recovery in the gas phase, especially in the Lower Aquifer. This implies that even in an initially water saturated aquifer, the gas phase may extend beyond the steam zone. Two mechanisms are responsible for the emergence of a gas phase ahead of the steam condensation front: (i) the development of a heated zone downstream from this front; and (ii) enhanced vaporization or even boiling of the more volatile NAPL components in the heated zone. Figs. 6-7 show that, as one might expect, the prominence of this feature increases with volatility of the organic compound -- it is more pronounced for the more volatile benzene than for p-xylene, and it is almost absent for n-decane.

Cumulative recoveries of the hydrocarbon components are shown in Figs. 9-11 and Fig. 12 shows the fractional recovery of hydrocarbon components from Layers 1 and 3 within each phase. As indicated earlier, initial conditions in Layers 1 and 3 are different. Layer 3 was initially saturated with water, whereas Layer 1 was only partially saturated. Moreover, NAPL was initially present in Layer 1 only in the immediate area around the producer, that is the initial average NAPL saturation in Layer 1 was significantly less than that in Layer 3. This is why these two layers respond differently to steam injection. With the exception of some benzene recovered in the aqueous phase, almost all contaminant recovery from Layer 1 is in the gas phase. Because this layer has a high initial gas saturation, gas is able to move toward the producer soon after injection starts, evaporating hydrocarbon components along the way. This continues throughout the injection period. Another reason for the dominance of gas phase recovery is that the total volume of NAPL initially present in Layer 1 is insufficient to sustain a mobile NAPL bank. Therefore, even when a NAPL bank forms, it eventually evaporates into the mobile gas phase recovered at the producer. The situation is different for the initially water-saturated Layer 3. Recovery in the gas phase accounts for 55%, 84%, and 91% respectively, of the total benzene, p-xylene, and n-decane recovered from Layer 3. Recovery in the water phase accounts for 22% of the total benzene and 2% of the total p-xylene recovered. Because of its low aqueous solubility, no significant amount of n-decane is recovered in the water phase. Twenty-three percent of the benzene, 14% of the p-xylene, and 9% of the n-decane recovered from Layer 3 are recovered as NAPL. These results are consistent with the most important interphase mass transfer characteristics of the components: the saturated vapor pressures and aqueous solubilities. Since the initial NAPL saturation is less than residual everywhere, recovery in the NAPL phase

must be preceded by the formation of a NAPL bank as described above. The NAPL bank is richer in the more volatile components because distillation favors such enrichment. Therefore fractional recovery as NAPL should be highest for the most volatile compounds still present in the gasoline.

The simulation results indicate that after 16 days of steam injection no free-phase gasoline is left in the permeable layers. Aqueous phase concentrations of benzene in these layers become very low, less than 0.01 mg/l everywhere. On the other hand, conditions in the Aquitard do not change from what they were initially. There is some increase in temperature due to thermal conduction, up to about 70°C near the injector. Free-phase gasoline initially present in the Aquitard remains after the 16 days of steam injection. As observed at the Clean Site, the low permeability of the Aquitard does not allow any significant amount of steam to enter and flow through it. Therefore, it has been decided [7] that gasoline recovery from the Aquitard will be achieved by resistance heating and vacuum extraction. Resistance heating will be used to dry up the Aquitard, creating a continuous and therefore mobile gas phase. This aspect of the remediation plan is not included in the work presented here.

The rates of steam injection into the Upper- and Lower Aquifer are shown in Fig. 13. As indicated earlier, the injection is pressure-constrained. In both layers, the rate of injection is highest at the beginning because the formation pressure is lowest at that time. As steam injection continues, the formation pressure increases, and the difference between the wellbore pressure and the formation pressure diminishes. This in turn leads to a decrease in the rate of steam injection. It should be noted that the cyclic variations or oscillations in the injection rates seen in Fig. 13 are caused by the rather coarse spatial discretization in the numerical simulations. A comparison of Figs. 13a and 13b shows that the cyclic variations are only significant for injection into an initially water-saturated medium. In multiphase flow problems that also involve phase change, calculated grid block pressures undergo cyclic variations as phase conditions in grid blocks change [1,3]. Consider how the steam condensation front is propagated in the finite-difference grid within Layers 3 and 4 (the Lower Aquifer). As water vapor enters a grid block that is just downstream from the steam front, it condenses, raising the temperature of this grid block. Eventually, this temperature reaches the boiling point of water at the prevailing pressure and the entire grid block makes a transition a two-phase condition. Water vapor continues to enter the grid block, condensing in part, and in part increasing gas saturation. The enthalpy of condensation goes to increase the temperature and pressure in the grid block, while steam mobility increases with saturation. At some point the steam begins to flow to the next downstream grid block where the process is repeated. The pressure variation described here propagates backward through the steam zone, causing the oscillation of the steam injection rate shown in Fig. 13. This oscillation is eventually dampened out by the high compressibility of the steam zone between the injection well and the condensation front.

The total rate of water production is shown in Fig. 14. During the first four days, almost all the water is produced from the Lower Aquifer. The initial mobility of water in the Upper Aquifer is low because this unit is unsaturated (the specified initial water saturation in this layer is 0.2, the irreducible saturation is 0.1). During this period, steam injected into the Upper Aquifer layer condenses, raising the water saturation there. Water production from the Upper Aquifer becomes significant after about four days of steam injection, and increases until the condensation front breaks through at about 7 days. Following this breakthrough, steam injected into the Upper Aquifer is produced with little condensation taking place. Because steam is less dense than water, the mass rate of production from the Upper Aquifer decreases. The production rate drops again after about 12 days of steam injection. This coincides with the time of breakthrough in the Lower Aquifer, and is also due to the difference in density between liquid water being produced prior to breakthrough and steam that is produced after it.

The total mass of steam injected during the 16-day simulation is 2200 m^3 of cold water equivalent (CWE) for the entire 7-spot pattern. Seventy-five percent of this amount is injected into the Upper Aquifer and the remainder into the Lower Aquifer. In principle, it is possible to reduce the mass of injected steam if injection into the Upper Aquifer is stopped soon after steam breakthrough there. The results of another simulation show that 1600 m^3 (CWE) of steam would be injected under that scenario. About 20% of the total injected heat is lost to the confining units.

Sensitivity Runs

A number of sensitivity runs were made to evaluate the influence of several key parameters on the results

presented above. In Sensitivity Run #1 the permeability of the sands and gravels units was changed from 5 to 10 darcy. As one would expect (Fig. 14), there is a nearly linear relationship between the time of steam breakthrough and permeability of the medium. The relative permeability of the NAPL was varied in Sensitivity Runs #2 and #3. In Run #2, the exponents for the two-phase NAPL relative permeabilities (n_{ow} and n_{og}) were changed from 1.5 to 2.0. In Sensitivity Run #3 the residual NAPL saturations (S_{orw} and S_{org}) were changed from 0.055 to 0.085. Results of both simulations show that the NAPL relative permeability can significantly affect the quantity of hydrocarbons recovered in the NAPL phase. Changes made here to the exponents and the residual NAPL saturation both have the effect of reducing the NAPL relative permeability. Therefore, the quantity of hydrocarbons recovered as NAPL in both simulations is significantly lower than that in the Base Run (Figs. 15-17). There is a corresponding increase in the quantity of hydrocarbons recovered in the gas phase. The overall recovery in all the phases shows very little sensitivity to these parameters, although the time to achieve a certain level of recovery may be somewhat different. Sensitivity Run #4 was designed to test the significance of the number of hydrocarbon components used to represent gasoline. Five hydrocarbon components were used in this run, compared to three used in the Base Run. The components used to represent gasoline in each of these two runs, and their mole fractions are shown in Table 2. A comparison of the simulation results is presented in Fig. 18. In terms of overall hydrocarbon recovery, there is no significant difference between the two simulations. However, there are differences in the amount of hydrocarbons recovered in each phase. A greater quantity of hydrocarbons is recovered in the gas and water phases in the Base Run than in Run #4. On the other hand, more separate-phase hydrocarbon is recovered in Run #4 than in the Base Run. The introduction of n-octane in Run #4 to represent some of the components approximated by p-xylene in the Base Run causes the saturation of the NAPL bank to be higher since n-octane is more volatile than p-xylene. This in turn increases separate-phase hydrocarbon recovery. The introduction of n-butylbenzene has the opposite effect since it is less volatile than n-decane. The substitution of n-octane for p-xylene has more impact than that of n-butylbenzene for n-decane. This is caused by a relatively higher differential of mole fractions and the saturated vapor pressures for the n-octane/p-xylene pair. A similar argument holds for the amount recovered in the water phase. The solubility of n-octane is much less than that of p-xylene, so that the net effect is a lower recovery in the water phase in Run #4. Since the bulk of recovery in the gas phase (especially in an initially water-saturated medium) comes after what is recovered as NAPL, a higher quantity of the latter implies a lower recovery in the gas phase (Fig. 18b). As was the case for the Clean Site Model, the simulation results presented here show little sensitivity to the choice of capillary pressure functions. The dominant recovery mechanisms are interphase mass transfer and viscous flow of the fluid phases.

Conclusions

A simulation model was developed to evaluate the potential for using steam injection to clean up gasoline contamination at the Gasoline Spill Area at LLNL. The results show that gasoline present in the permeable sands and gravel layers can be successfully recovered by injecting steam into those layers in a 7-spot pattern. For the conditions assumed in the model, it will take less than 16 days to recover nearly all of the gasoline in the sands and gravel layers. By that time, the maximum aqueous concentrations of hydrocarbon components in these layers will have dropped to less than 0.01 mg/l.

The results show that vaporization, followed by bulk movement of the vapor to the production well is the dominant recovery mechanism. In terms of time required for cleanup, model results are most sensitive to permeability of the medium. Other parameters, such as the relative permeabilities also affect the outcome, but to a lesser extent.

Although the simulations described in this paper are predictive, in the sense that there is no historical data for comparison, the reasonable and continuous dependence of the results on input data provides another indication that the M^2NOTS simulator is 'well behaved.'

References

1. Pruess, K., TOUGH User's Guide, Nuclear Regulatory Commission, Report NUREG/CR-4645, 1987.

2. Pruess, K., TOUGH2 -- A General Purpose Numerical Simulator for Multiphase Fluid and Heat Flow, Lawrence Berkeley Laboratory Report LBL-29400, Berkeley, CA 1990.

3. Adenekan, A. E., Numerical Modeling of Multiphase Transport of Multicomponent Organic Contaminants and Heat in the Subsurface, Ph.D. Dissertation, University of California, Berkeley, 1992.

4. Adenekan, A. E., Patzek, T. W. and Pruess, K., Modeling of Multiphase Transport of Multicomponent Organic Contaminants and Heat in the Subsurface, I. Model Formulation, submitted to *Water Resources Research*, 1992.

5. Adenekan, A. E., Patzek, T. W. and Pruess, K., Modeling of Multiphase Transport of Multicomponent Organic Contaminants and Heat in the Subsurface, II. Model Verification, submitted to *Water Resources Research*, 1992.

6. Hunt, J. R., Sitar, N. and Udell, K. S., Nonaqueous phase liquid transport and cleanup, 2. Experimental Studies, *Water Resources Research* **24** 8 1259-1269, 1988.

7. Aines, R. (Editor), Dynamic Underground Stripping Demonstration Project, Interim Report, Lawrence Livermore National Laboratory Report No. UCRL-ID-109906, March, 1992.

8. Thorpe, R. K., W. F. Isherwood, M. D. Dresen, and C. P. Webster-Scholten (Editors), CERCLA Remediation Investigations Report for the LLNL Livermore Site, Lawrence Livermore National Laboratory, Livermore, CA., UCRL-AR-10299, 1990.

9. Nichols, E. M., M. D. Dresen, and J. E. Field, Proposal for Pilot Study at LLNL Building 403 Gasoline Station Area, Lawrence Livermore National Laboratory Environmental Restoration Series, UCAR-10248, August 1988.

10. Parker, J. C., Lenhard, R. J., and Kappusamy, T., A Parametric Model for Constitutive Properties Governing Multiphase Fluid Flow in Porous Media, *Water Resources Research* **23** 4 618-624, 1987.

11. Kreamer, D. K. and K. J. Stetzenbach, Development of a standard, pure-compound base gasoline mixture for use as a reference in field and laboratory experiments, *Groundwater Monitoring Review*, Spring 1990.

12. Johnson, P. C., M. W. Kemblowski, and J. D. Colthart, Quantitative analysis for cleanup of hydrocarbon-contaminated soils by in-situ soil venting, *Groundwater*, **28**(3), 413-429, 1990.

13. Weiss Associates, Personal communication, 1992.

Table 1: Rock Properties used in the Base Run

	Sands and Gravels	Silts and Clays
Permeability	5.0×10^{-12} m^2	1.0×10^{-14} m^2
Porosity	0.25	0.25
Soil grain density	2650 kg/m^3	2650 kg/m^3
Soil grain specific heat capacity	720 J/kg·K	720 J/kg·K
Dry media thermal conductivity	0.50 W/m·K	1.50 W/m·K
Liquid saturated thermal conductivity	3.10 W/m·K	3.10 W/m·K
Residual NAPL saturation, $S_{orw} = S_{org}$	0.055	0.085
Irreducible water saturation, S_{wir}	0.10	0.15
Residual gas saturation, S_{gr}	0.01	0.01
$n_{ow} = n_{og}$	1.5	1.5
n_w	2.0	2.0
n_g	1.2	1.2
k_{rwro}	0.8	0.8
k_{rocw}	1.0	1.0
k_{rgro}	1.0	1.0
n	5.0	3.0
α_{go}	40.0	6.0
α_{ow}	40.0	6.0
S_m	0.0	0.0

Two-phase water-oil and oil-gas relative permeability functions:

$$k_{rw} = k_{rwro}\left[\frac{S_w - S_{wir}}{1 - S_{orw} - S_{wir}}\right]^{n_w}$$

$$k_{row} = k_{rocw}\left[\frac{1 - S_w - S_{orw}}{1 - S_{orw} - S_{wir}}\right]^{n_{ow}}$$

$$k_{rog} = k_{rocw}\left[\frac{1 - S_{wir} - S_{org} - S_g}{1 - S_{wir} - S_{org}}\right]^{n_{og}}$$

$$k_{rg} = k_{rgro}\left[\frac{S_g - S_{gr}}{1 - S_{wir} - S_{org} - S_{gr}}\right]^{n_g}$$

Two-phase water-oil and oil-gas capillary pressure functions:

$$P_{cow} = \frac{\varrho_w g}{\alpha_{ow}}\left(\left(\frac{S_w - S_m}{1 - S_m}\right)^{-1/m} - 1\right)^{1/n}$$

$$P_{cgo} = \frac{\varrho_w g}{\alpha_{go}}\left(\left(\frac{S_w + S_o - S_m}{1 - S_m}\right)^{-1/m} - 1\right)^{1/n}$$

where $m = 1 - 1/n$.

Table 2: Pseudocomponents used to represent gasoline

Base Run: 3 Pseudocomponents
1. Benzene. Mole fraction = 0.022; represents Benzene
2. p-Xylene. Mole fraction = 0.741; represents all C_7—C_9 hydrocarbons
3. n-Decane. Mole fraction = 0.237; represents all C_{10}— C_{12} hydrocarbons
Sensitivity Run #4: 5 Pseudocomponents
1. Benzene. Mole fraction = 0.022; represents Benzene
2. p-Xylene. Mole fraction = 0.497; represents C_7—C_9 aromatics
3. n-Octane. Mole fraction = 0.233; represents C_7—C_9 paraffins, olefins, etc.
4. n-butylbenzene. Mole fraction = 0.168; represents C_{10}—C_{11} aromatics
5. n-Decane. Mole fraction = 0.080; represents all C_{10}— C_{12} hydrocarbons

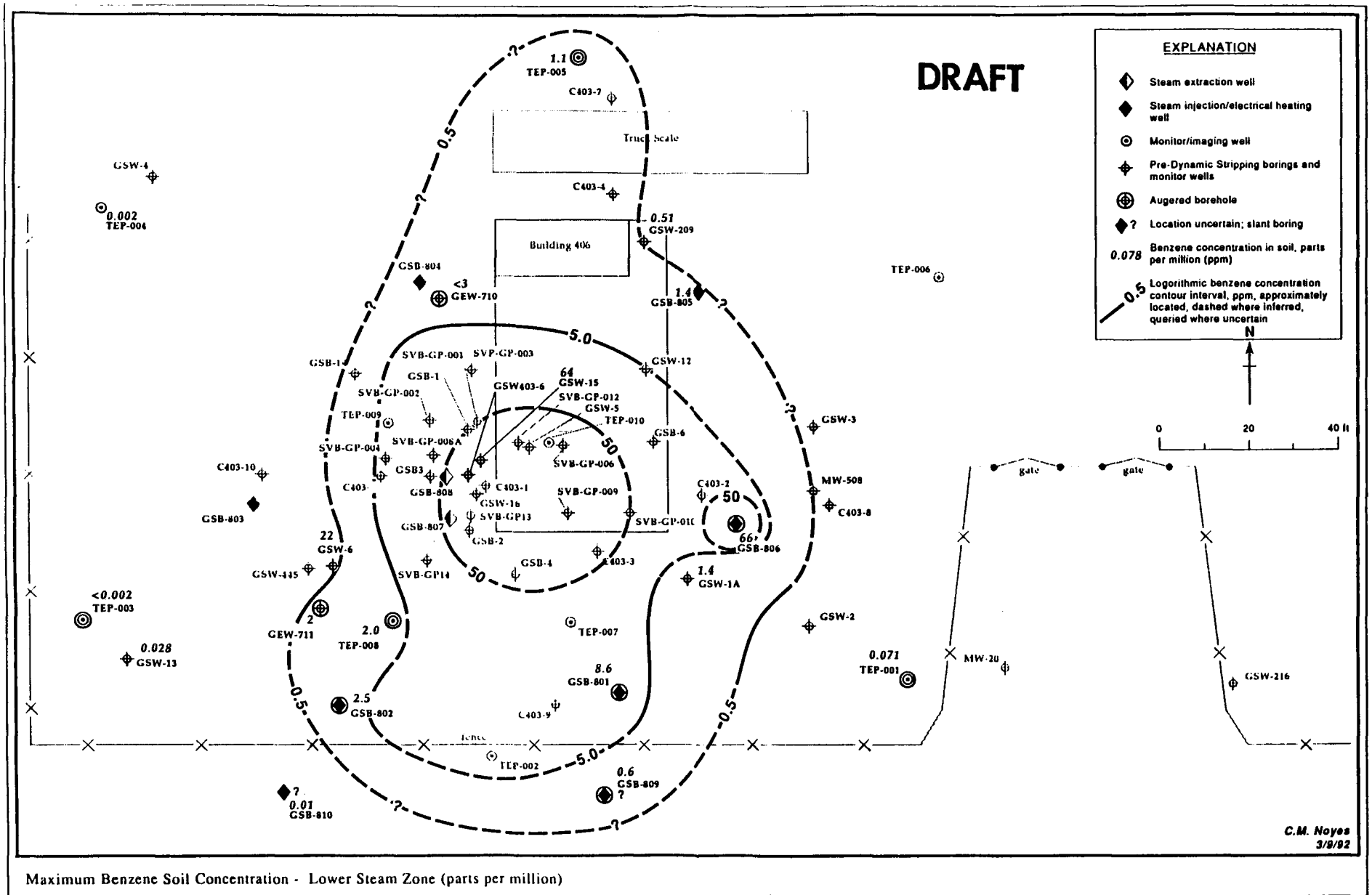

Fig. 1. Plan view of the Gasoline Spill Area.

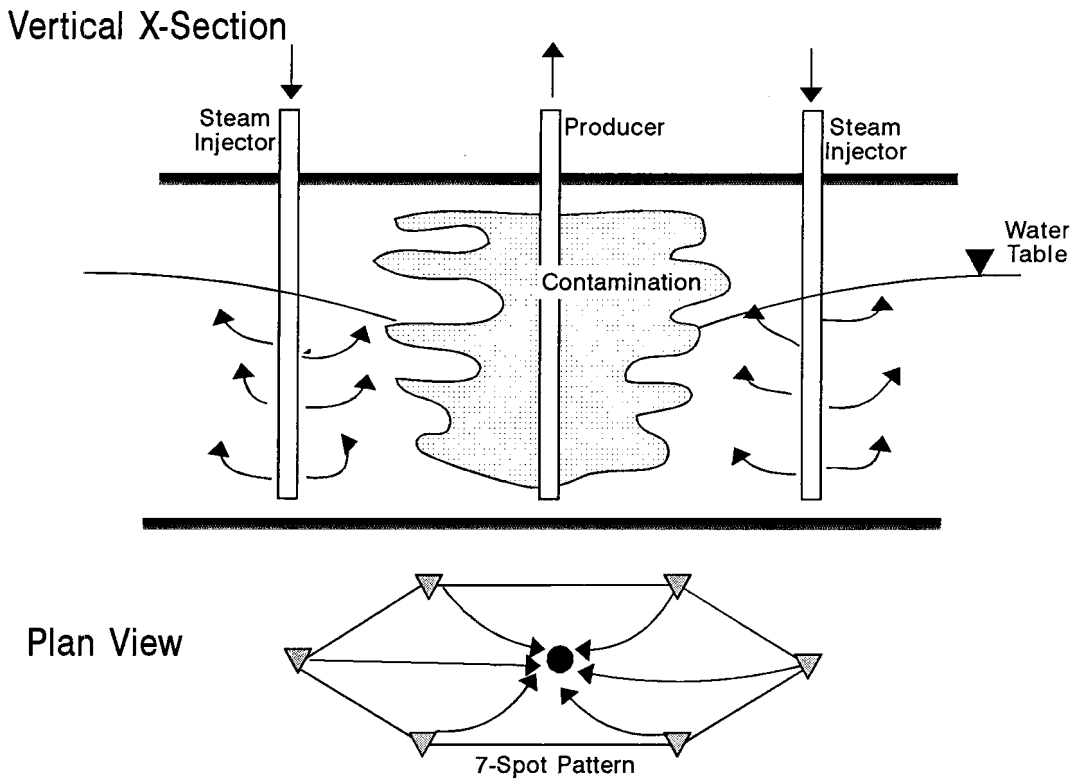

Fig. 2. 7-spot pattern.

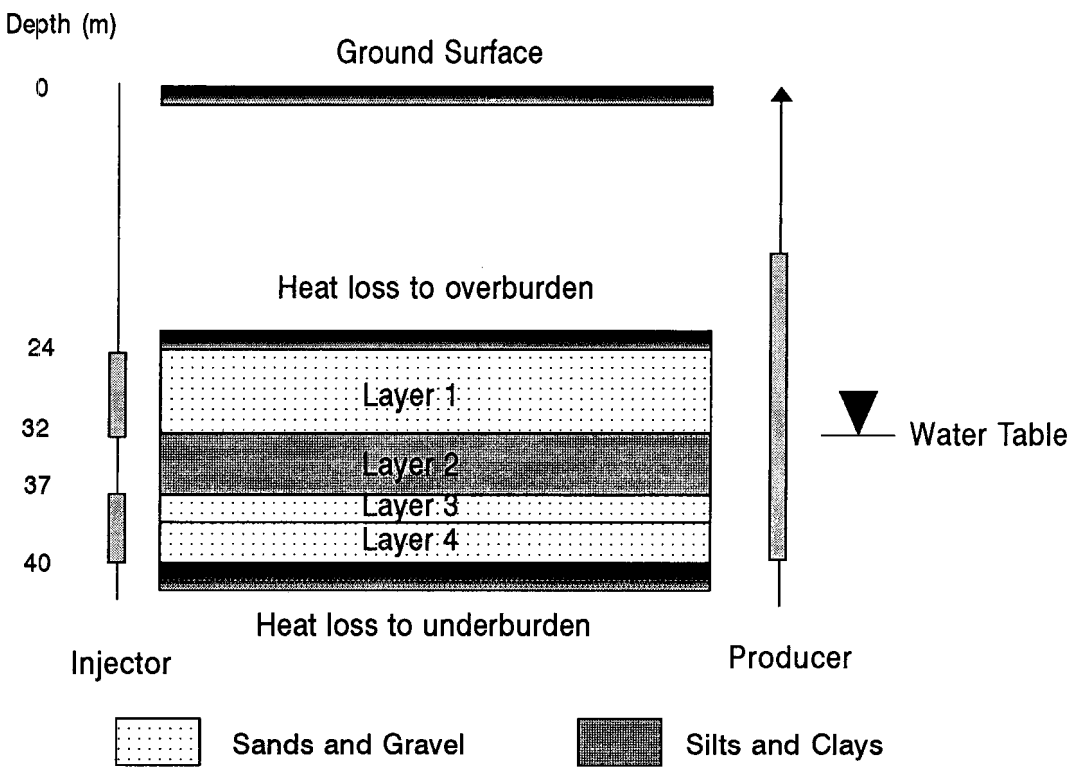

Fig. 3. Vertical cross-section of finite-difference grid.

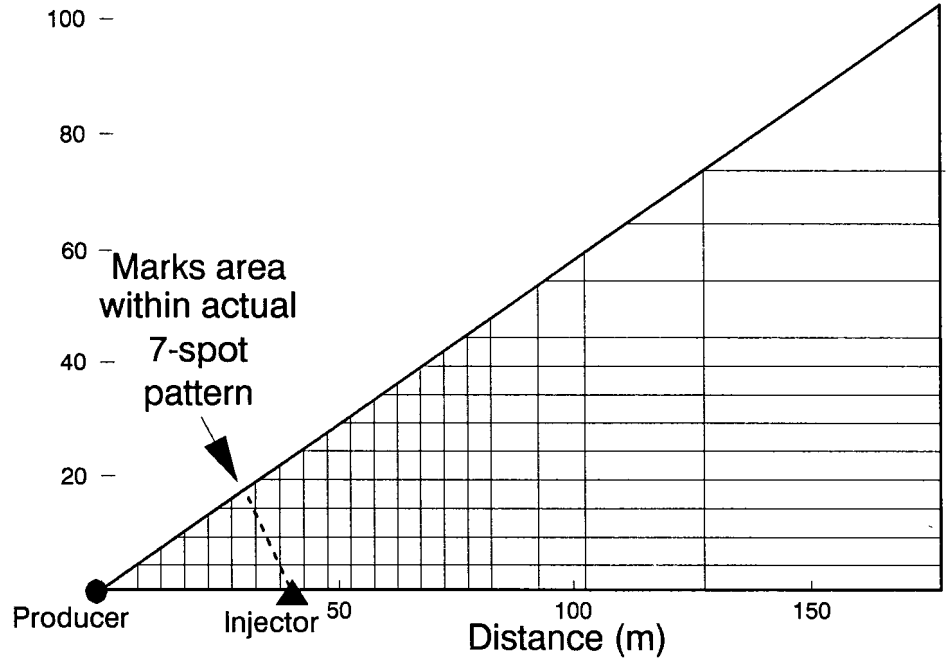

Fig. 4. Plan view of finite-difference mesh.

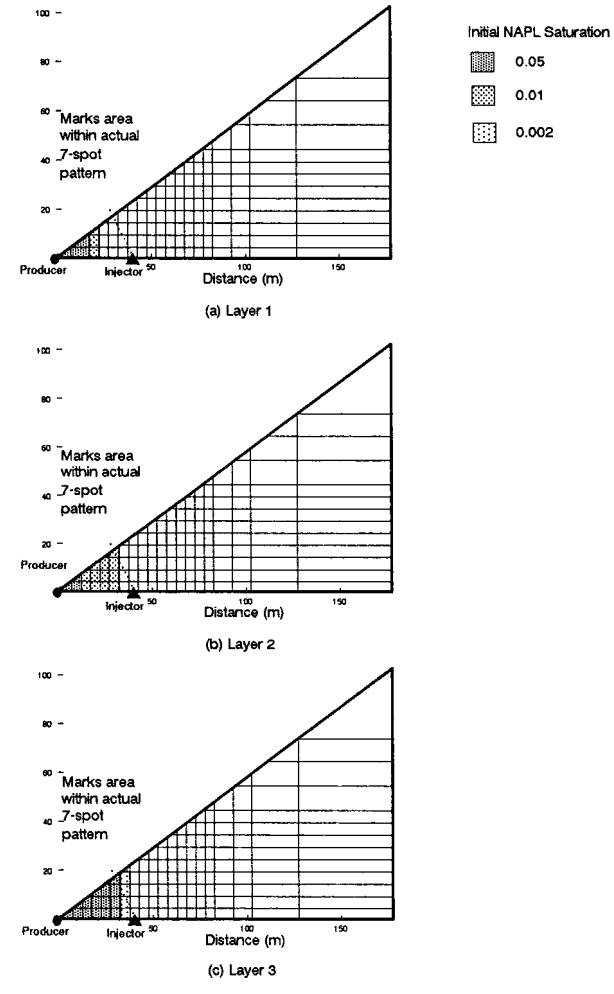

Fig. 5. Initial distribution of gasoline.

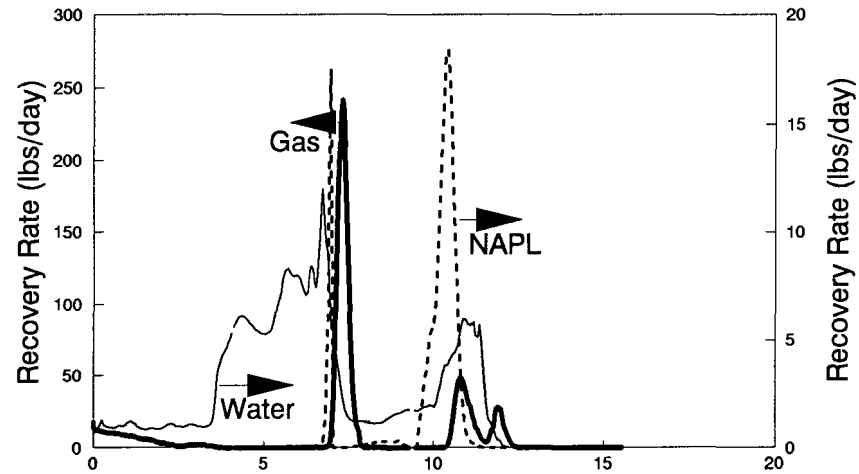

Fig. 6. Benzene recovery rates per 1/12 of 7-spot pattern.

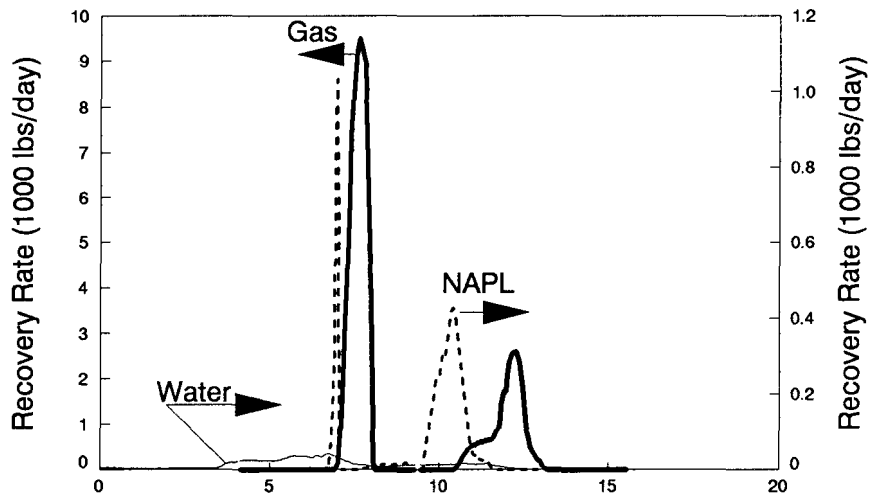

Fig. 7. P-xylene recovery rates per 1/12 of 7-spot pattern.

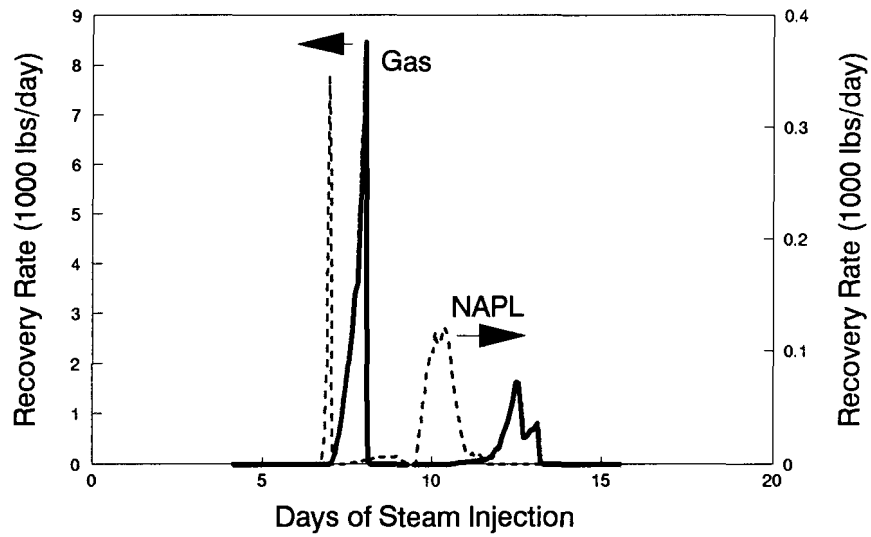

Fig. 8. N-decane recovery rates per 1/12 of 7-spot pattern.

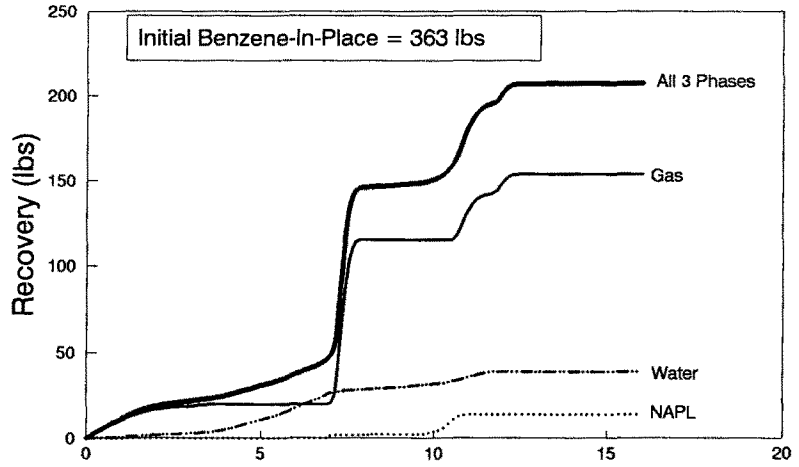

Fig. 9. Cumulative recovery of benzene per 1/12 of 7-spot.

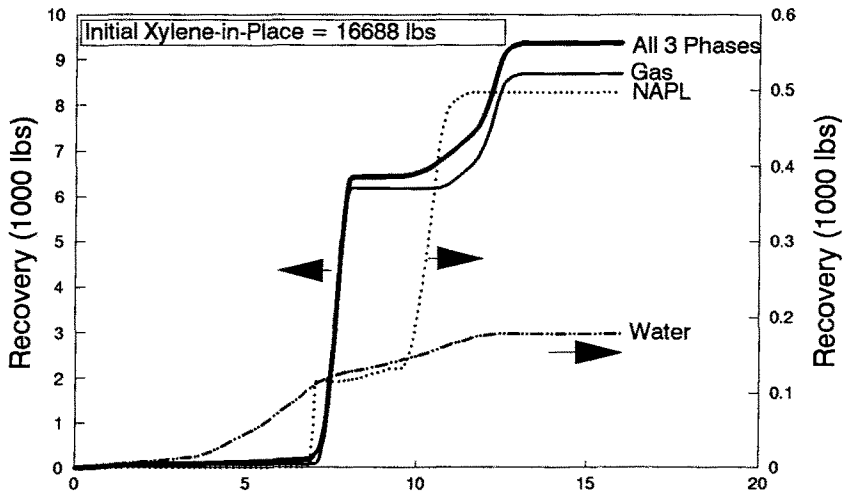

Fig. 10. Cumulative recovery of p-xylene per 1/12 of 7-spot.

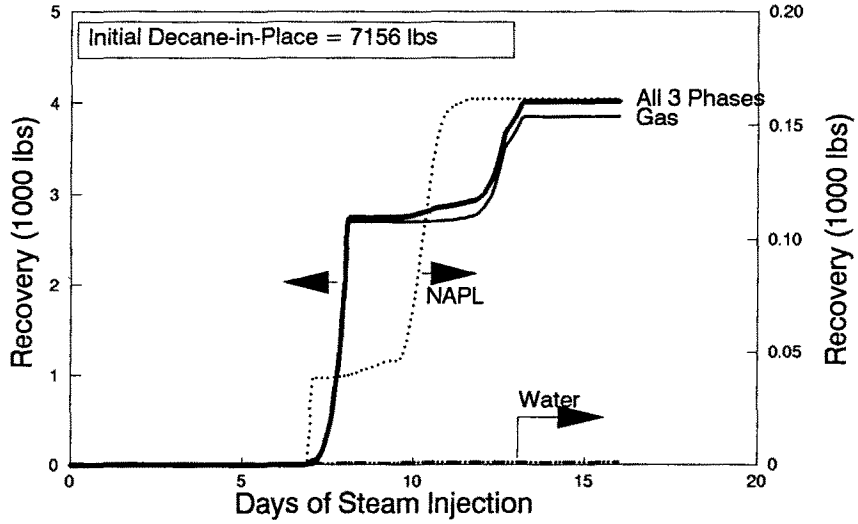

Fig. 11. Cumulative recovery of n-decane per 1/12 of 7-spot.

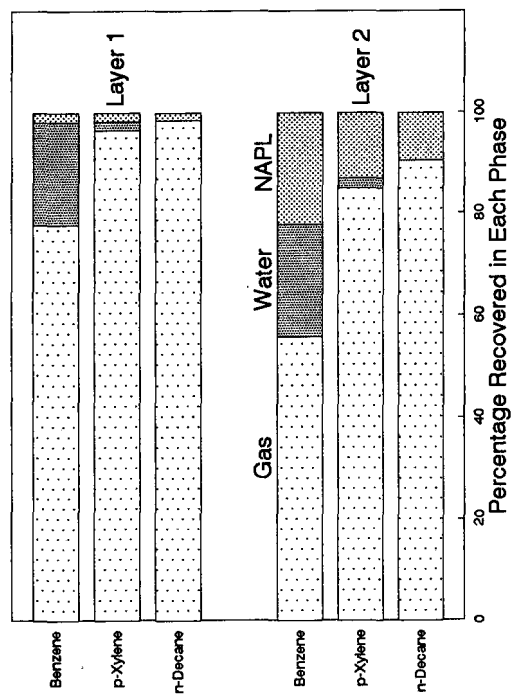

Fig. 12. Relative hydrocarbons recoveries.

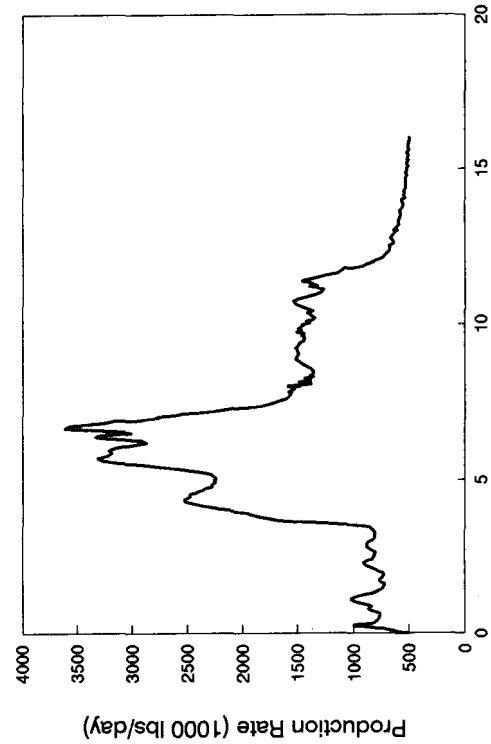

Fig. 14. Water production rate.

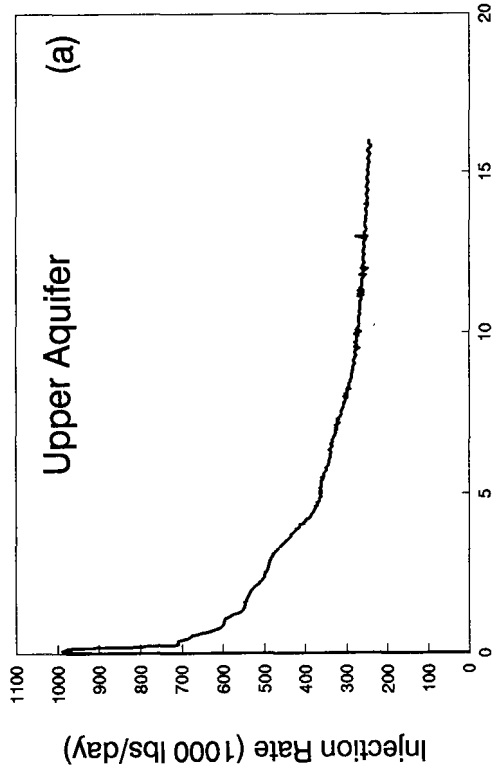

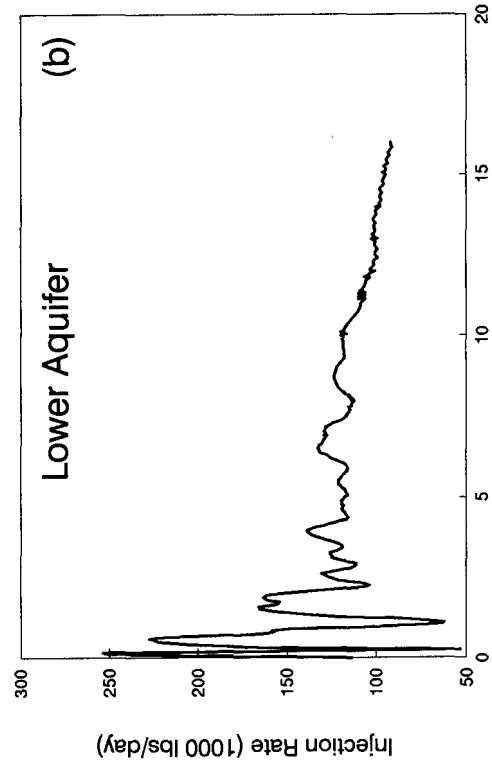

Fig. 13. Steam injection rates.

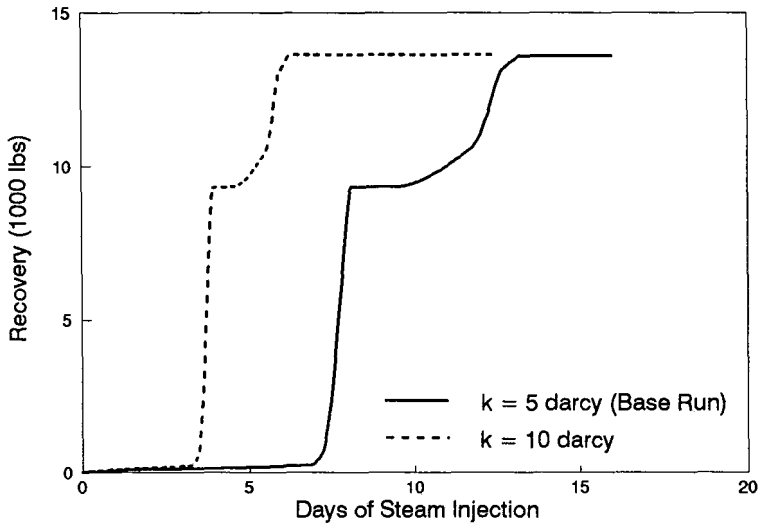

(a) Recovery of all components in all phases

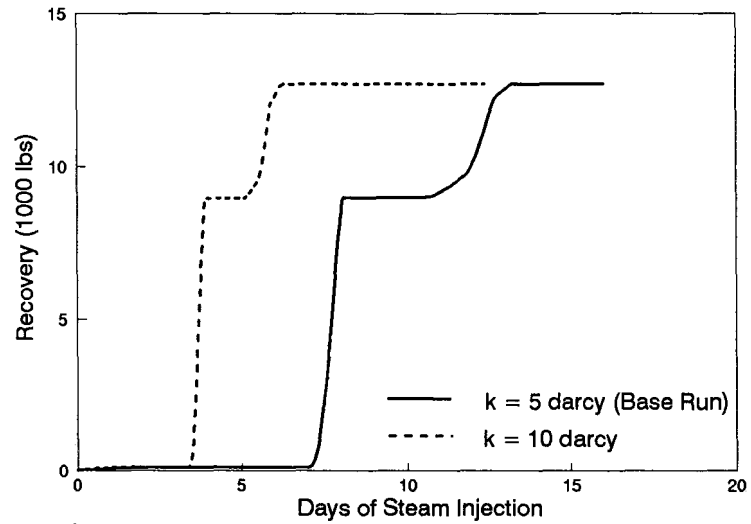

(b) Recovery of all components in the gas phase

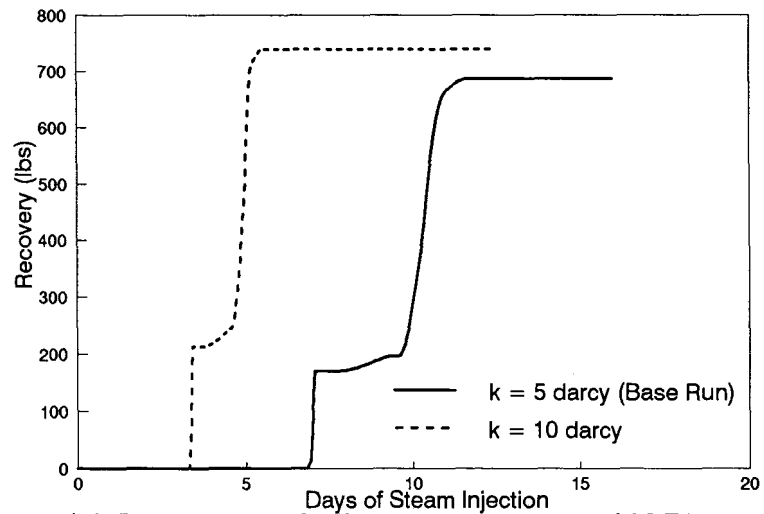

(c) Recovery of all components as NAPL

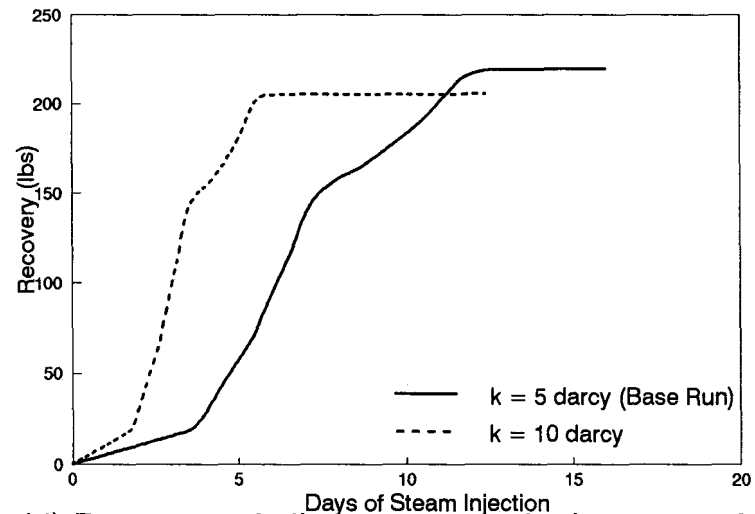

(d) Recovery of all components in the water phase

Fig. 15. Sensitivity Run #1.

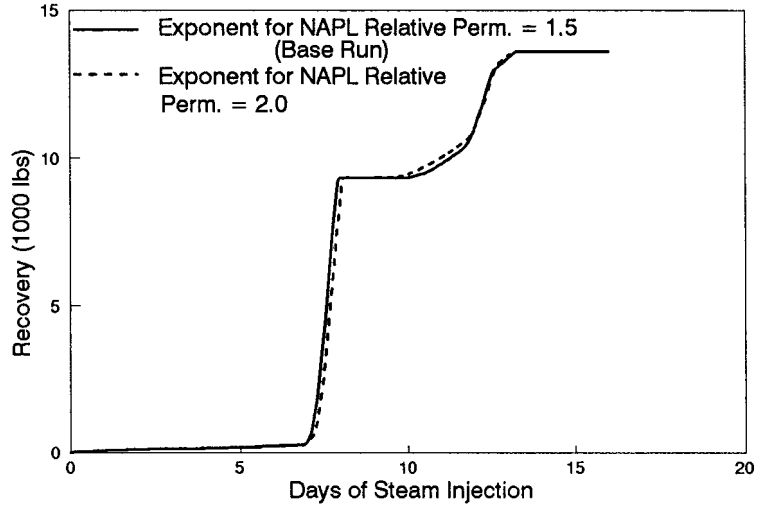

(a) Recovery of all components in all phases

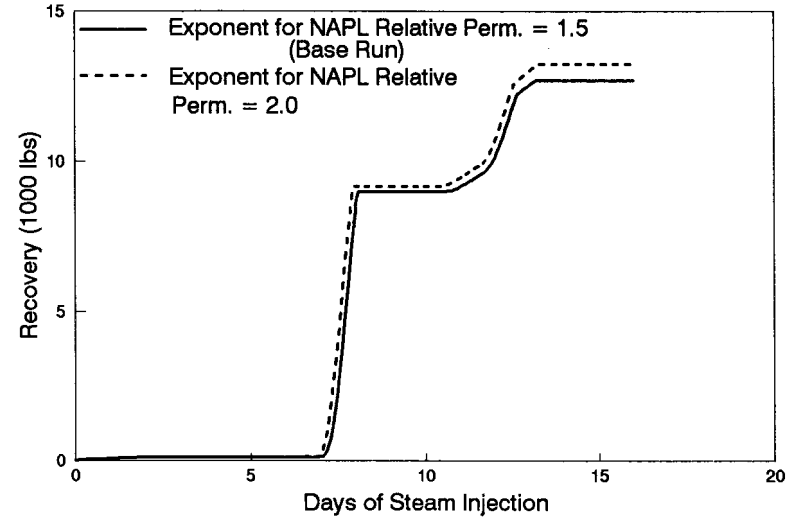

(b) Recovery of all components in the gas phase

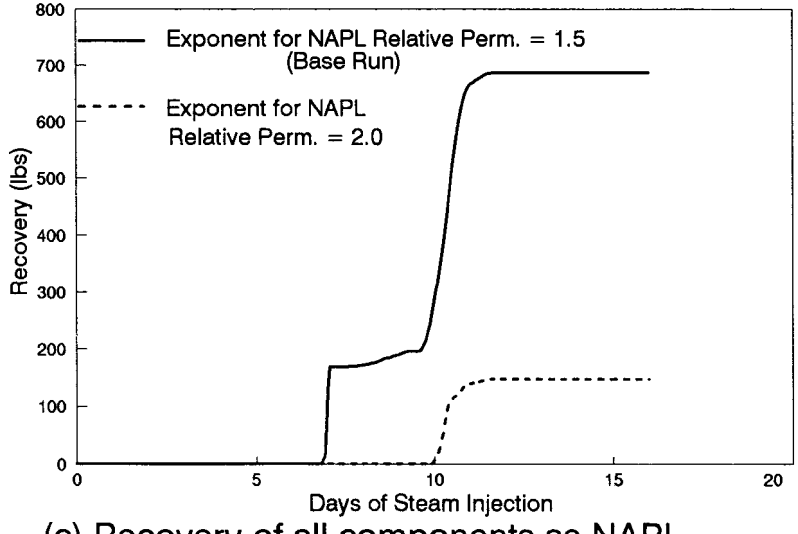

(c) Recovery of all components as NAPL

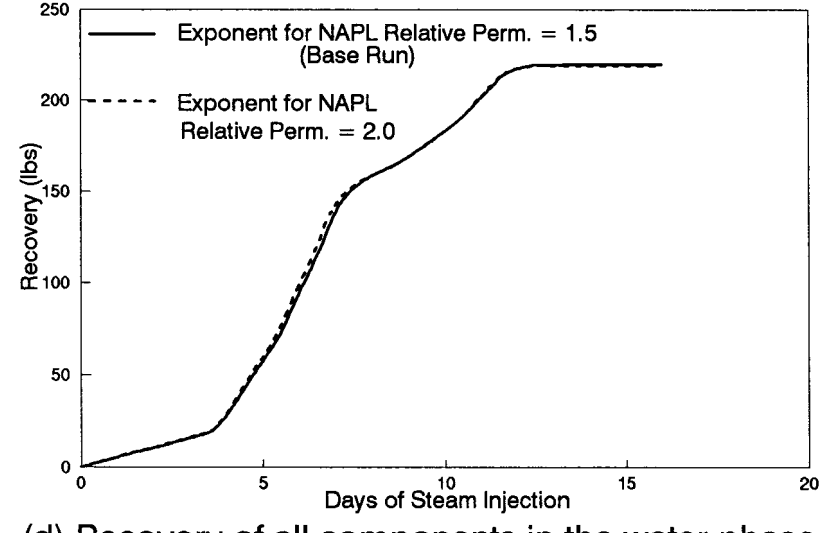

(d) Recovery of all components in the water phase

Fig. 16. Sensitivity Run #2.

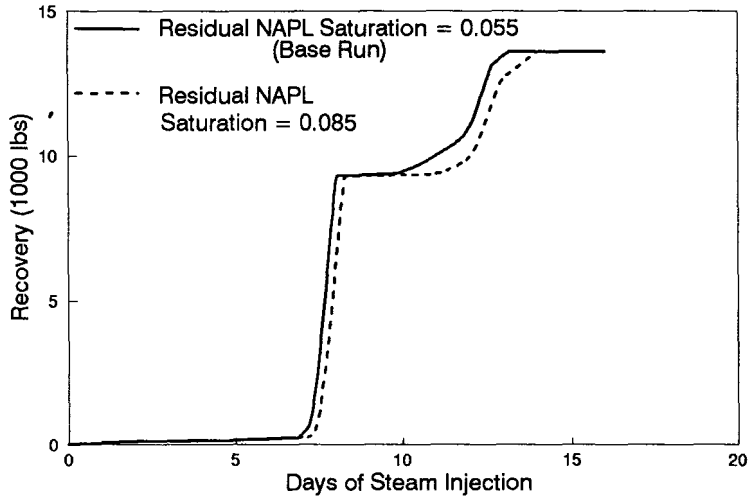

(a) Recovery of all components in all phases

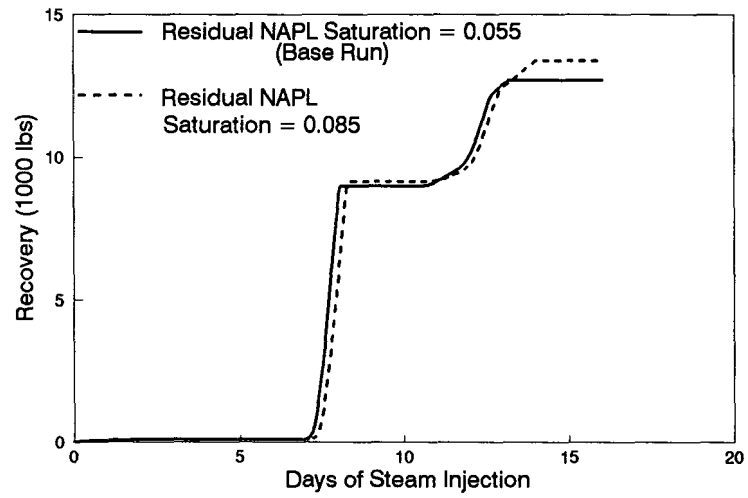

(b) Recovery of all components in the gas phase

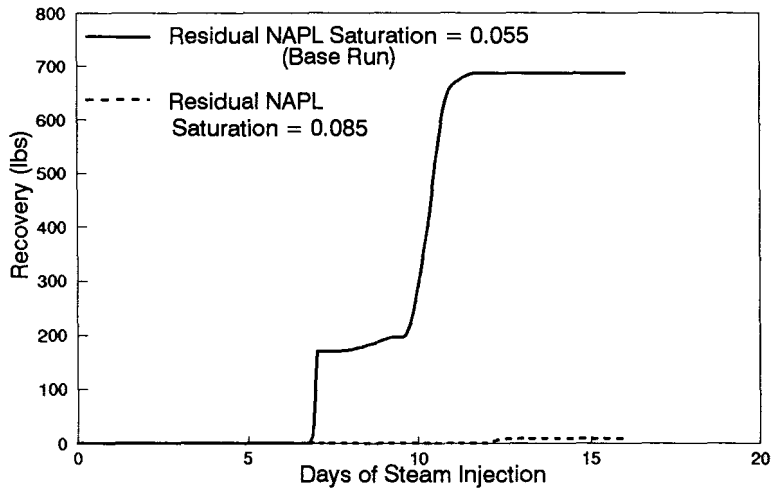

(c) Recovery of all components as NAPL

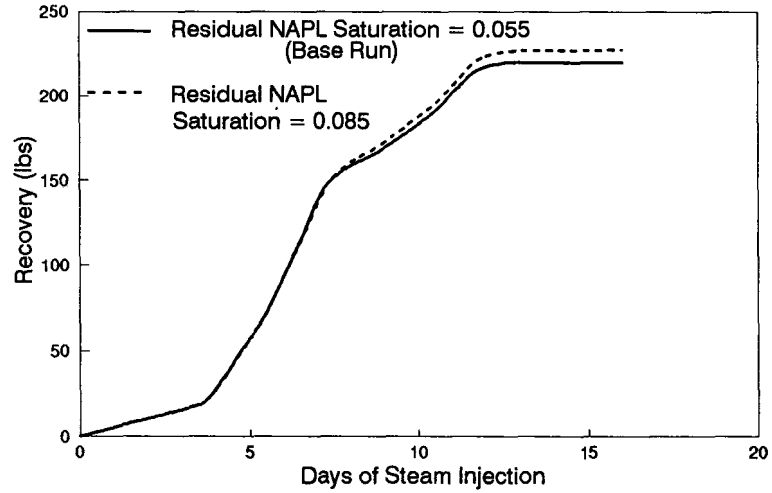

(d) Recovery of all components in the water phase

Fig. 17. Sensitivity Run #3.

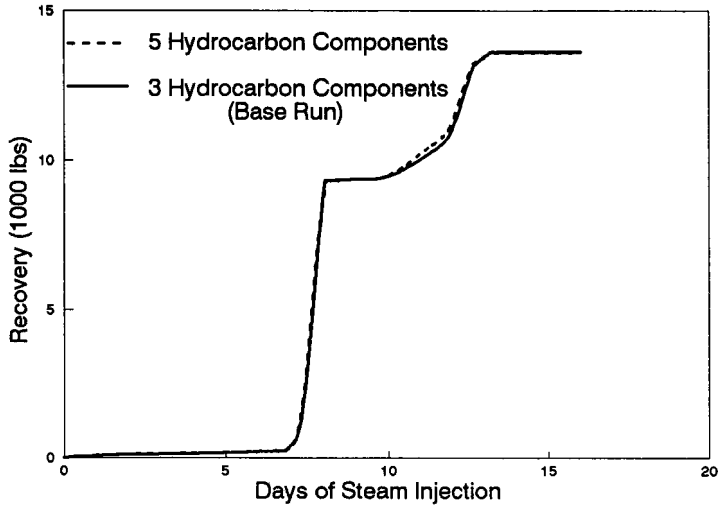

(a) Recovery of all components in all phases

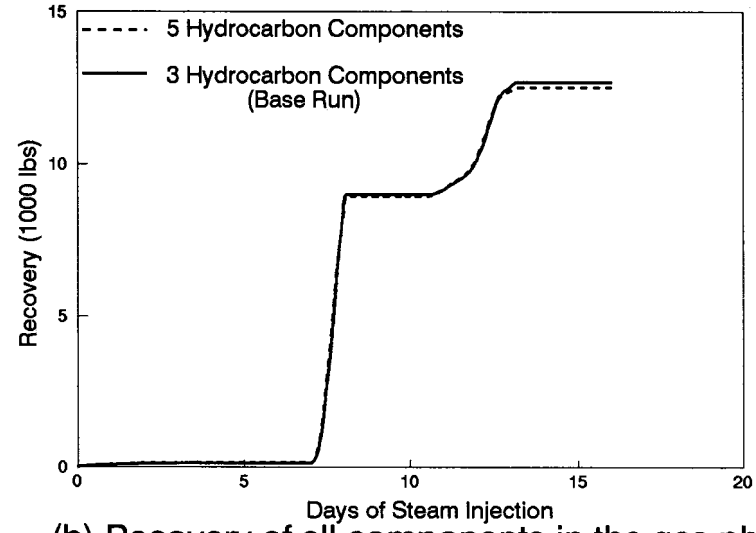

(b) Recovery of all components in the gas phase

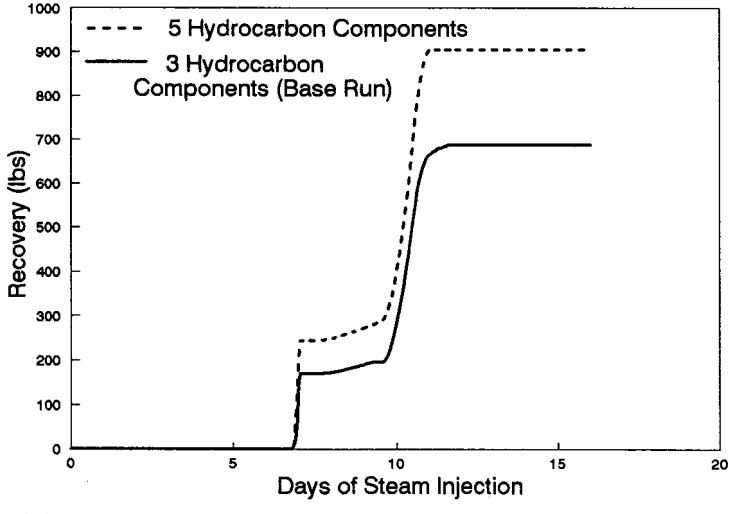

(c) Recovery of all components as NAPL

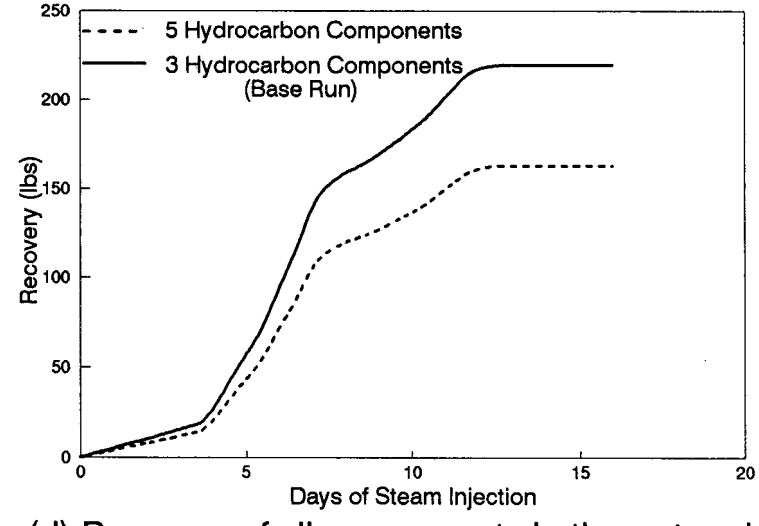

(d) Recovery of all components in the water phase

Fig. 18. Sensitivity Run #4.